Loss of Bone Morphogenetic Protein-binding Endothelial Regulator Causes Insulin Resistance

Hua Mao[1,2], Luge Li[1,2], Qiying Fan[1,2], Aude Angelini[1,2], Pradip K. Saha[3], Huaizhu Wu[1,2], Christie M. Ballantyne[1,2], Sean M. Hartig[3,4], Liang Xie[1,2], Xinchun Pi[1,2*]

[1]Department of Medicine, Section of Athero & Lipo, Baylor College of Medicine, Houston, TX

[2]Cardiovascular Research Institute, Baylor College of Medicine, Houston, TX

[3]Department of Medicine, Division of Diabetes, Endocrinology & Metabolism, Diabetes Research Center, Baylor College of Medicine, Houston, TX

[4]Departments of Molecular and Cellular Biology, Baylor College of Medicine, Houston, TX

Corresponding author:

Xinchun Pi, Ph.D.

Cardiovascular Research Institute and Department of Medicine

Baylor College of Medicine

Houston, TX 77030

Tel: +1 713 798 5984

Email: xpi@bcm.edu

Accumulating evidence suggests chronic inflammation of metabolic tissues plays a causal role in obesity-induced insulin resistance. Yet, how specific endothelial factors exert impacts in metabolic tissues remains undefined. Bone morphogenetic protein (BMP)–binding endothelial regulator (BMPER) adapts endothelial cells to inflammatory stress in diverse organ microenvironments. Here we demonstrate BMPER is a driver of insulin sensitivity. Inducible knockout (iKO) of BMPER causes hyperinsulinemia, glucose intolerance and insulin resistance without increasing inflammation in metabolic tissues. Interestingly, BMPER can directly activate insulin signaling, which requires its internalization and interaction with Niemann-Pick C1 (NPC1), an integral membrane protein that transports intracellular cholesterol. These results suggest the endocrine function of the vascular endothelium maintains glucose homeostasis. Of potential clinical significance, the delivery of BMPER recombinant protein or its overexpression significantly alleviates insulin resistance and hyperglycemia in high-fat diet (HFD)-fed mice and Lepr$^{db/db}$ (*db/db)* diabetic mice. We conclude that BMPER exhibits therapeutic potential for the treatment of diabetes.

Diabetes mellitus (DM) is a group of metabolic diseases characterized by chronic hyperglycemia and impaired carbohydrates, lipids and protein metabolism resulting from defects in insulin secretion, insulin action or both. More than 100 million U.S. adults are now living with diabetes or prediabetes, a condition that if not treated often leads to type 2 diabetes mellitus (T2DM) within five years[1]. T2DM is the most common form of DM, accounting for 90% to 95% of all diabetic patients and is expected to increase to 693 million by 2045[2]. T2DM is associated with an increased risk of micro- and macrovascular complications, such as diabetic nephropathy, neuropathy, retinopathy and coronary artery disease, which impose profound impacts on the quality of life and health care resources. Current management of diabetes includes lifestyle intervention, routine blood glucose monitoring and pharmacological therapy. However, high costs, variable efficiency and tolerability are important barriers to the use of these pharmacological treatments.

Insulin resistance is a core defect of T2DM and associated with chronic inflammatory responses. During chronic inflammation, macrophage plays a crucial role in obese-induced insulin resistance[3,4]. After microphages are infiltrated into metabolic tissues such as obese adipose tissue, their secreted pro-inflammatory cytokines inhibit insulin signaling and result in insulin resistance. Another key player of chronic inflammation is vascular endothelium, which coordinates the action of immune cells through the continual adjustment in its own structure and function, including induction of adhesion molecules and pro-inflammatory cytokines, disruption of its barrier function and angiogenesis[5]. Even though endothelial dysfunction and inflammation have been observed during the development of T2DM[6,7], it remains unknown whether endothelial cells (ECs) play a crucial role in the maintenance of glucose homeostasis and how its dysregulation contributes to insulin resistance and diabetes.

BMP pathway is known as an important regulator in the maintenance of endothelial integrity and the induction of vascular inflammatory responses[8]. BMPER (also called CV-2) binds BMPs and is an extracellular modulator of BMP signaling pathway[9]. We have discovered BMPER plays a pivotal role in BMP-mediated endothelial events and chronic inflammation in the vasculature[10-15]. However, the role of BMPER in obesity and insulin resistance has not been studied before.

In this study, we have made a surprising observation that BMPER regulates glucose homeostasis without affecting chronic inflammation. Instead, BMPER is a driver of insulin sensitivity through activating insulin signaling pathway in hepatocytes. This activation requires BMPER endocytosis and interaction with Niemann-Pick C1 (NPC1), an integral membrane protein that transports intracellular cholesterol[16,17]. Both whole-body and EC-specific BMPER inducible knockout (iKO) mice display similar glucose defects, including hyperinsulinemia, insulin resistance and glucose intolerance, suggesting vascular endothelium plays a causal role in glucose homeostasis through secreting metabolic regulators. More importantly, the delivery of BMPER recombinant protein or its adeno-associated viral (AAV) particles dramatically alleviates insulin resistance and hyperglycemia in diabetic mice. Our data

reveal that BMPER is a protective regulator of glucose homeostasis and could become a potential therapeutic target for treating diabetes.

Results

Loss of BMPER results in glucose dysregulation. BMPER null mice die at birth due to lung defects[12], which limits our understanding of BMPER's functions during pathological conditions at adulthood. To study the role of BMPER in glucose homeostasis, we generated BMPER$^{flox/flox}$ mice using CRISPR-cas9 gene editing (Fig. 1a). A BMPER inducible knockout KO (iKO) mouse model was created by crossing BMPER$^{flox/flox}$ and CAG-CreER$^{+/-}$ transgenic mice (Fig. 1a), which allows temporal depletion of BMPER upon tamoxifen injection. BMPER depletion was confirmed in plasma and a variety of tissues of BMPER iKO compared to their littermate control (WT, BMPER$^{flox/flox}$; CAG-CreER$^{-/-}$) mice (Fig. 1b). Interestingly, BMPER iKO mice displayed hyperinsulinemia and higher homeostasis model assessment for insulin resistance (HOMA-IR) scores than WT mice at four months after tamoxifen injection (Fig. 1c-e, Supplementary Table 1). In addition, BMPER iKO mice were more glucose intolerant and insulin resistant (Fig. 1f-g). To further explore insulin sensitivity, hyperinsulinemic-euglycemic clamp studies were performed. As shown in Fig. 1h-i, the amount of exogenous glucose required for maintaining euglycemia (glucose infusion rate, GIR) and the glucose disposal rate (GDR) were markedly lower in BMPER iKO mice than WT mice. Both the ability of insulin to suppress hepatic glucose production, which reflects hepatic insulin sensitivity, and the insulin-stimulated glucose uptake in skeletal muscle, heart and brown adipose tissue, which reflects insulin sensitivity in peripheral tissues, were significantly decreased in BMPER iKO mice (Fig. 1j-k). We also evaluated the expression of liver genes that reflect glucose output. BMPER depletion led to a significant induction of gluconeogenic enzymes, including G6Pase (glucose-6-phosphatase) and PEPCK (phosphoenolpyruvate carboxykinase), and a lipogenic transcription factor SREBP1 (sterol regulatory element-binding transcription factor 1; Supplementary Fig. 1a). However, no change was observed with the glycolytic enzyme- glucokinase (GK;

Supplementary Fig. 1a). Taken together, these results suggest BMPER depletion results in glucose dysregulation through regulating insulin sensitivity, gluconeogenesis and lipogenesis.

Inflammation is not observed in BMPER iKO mice. Given that vascular inflammation also disrupts function of metabolic tissues such as liver and WAT[18-20], we examined whether BMPER depletion resulted in an inflammatory response in these tissues. In the liver of BMPER iKO and WT mice, the induction of the inflammatory cytokine IL1β (Supplementary Fig. 1b) was not changed while others- IL6 and TNFα were not detectable (data not shown). Their levels did not change in WAT either (Supplementary Fig. 1c). These results suggest that inflammation does not contribute to the disruption of glucose homeostasis by BMPER depletion.

BMPs play a role in obesity through regulating adipogenesis and energy storage partitioning[21-24], we asked whether BMPER also regulates body weight through modulating BMP signaling. Surprisingly, there was no body weight difference between BMPER iKO and WT mice (Supplementary Table 1). Further CLAMS (comprehensive lab animal monitoring system) studies demonstrated a decrease in respiration exchange ratio (RER), a mild increase in physical activity and a non-significant trend of increase in food intake of BMPER iKO mice compared to WT mice (Supplementary Fig. 2). In addition, we observed no significant changes with the expression of BMPs and BMP receptor 2 (BMPR2) in the liver of BMPER iKO mice compared to WT mice (Supplementary Fig. 1d). It suggests, unlike BMPs, BMPER does not play a significant role in body weight control.

Given that BMPER iKO mice spontaneously developed hyperinsulinemia, insulin resistance and glucose intolerance without weight gain (Fig. 1c-k, Supplementary Table 1), we hypothesized BMPER iKO mice are more sensitive to the metabolic effects of high-fat diet (HFD). Following eight weeks of HFD feeding, BMPER iKO and WT mice gained similar weight and displayed comparable glucose and insulin levels (Supplementary Fig. 3a-c). However, BMPER iKO mice exhibited more severe glucose intolerance and insulin resistance than WT mice (Supplementary Fig. 3d-e). These observations suggest BMPER depletion exacerbates obesity-induced insulin resistance and glucose intolerance.

Loss of BMPER in ECs results in glucose dysregulation. Our previous studies[10-15] suggest that BMPER is highly expressed in vascular endothelial cells (ECs). To determine whether EC is an important source for BMPER production, we generated endothelium-specific BMPER inducible knockout (eKO) mice by breeding BMPER$^{flox/flox}$ and Cdh5-CreER$^{+/-}$ mice. BMPER eKO mice, similarly to its global depletion (Fig. 1), displayed hyperinsulinemia, glucose intolerance and insulin resistance without weight difference compared to their littermate control (eWT, BMPER$^{flox/flox}$; Cdh5-CreER$^{-/-}$) mice (Supplementary Fig. 4). BMPER depletion in ECs also resulted in hepatic and peripheral insulin resistance (Supplementary Fig. 5). These data suggest EC is an important source for BMPER in periphery.

BMPER plasma level decreases in humans with metabolic syndrome. Since BMPER serum level was lower in BMPER iKO mice that spontaneously developed hyperinsulinemia and insulin resistance, we examined whether there is an association between BMPER level and insulin resistance. To this end, we observed that BMPER plasma level was reduced by ~50% in humans with metabolic syndrome (MS)[25], a complication often coupled with insulin resistance and increased risk for T2DM[26], compared to healthy individuals (Fig. 2a, b). In addition, BMPER levels negatively correlated with body weight and plasma levels of insulin and triglycerides (TG; Fig. 2c-f), suggesting an association between decreased BMPER levels and conventional serum markers of insulin resistance. Similarly, a ~70% decrease of BMPER plasma level was observed in high-fat diet (HFD)-fed mice (Fig. 2g-h). These results suggest that BMPER plasma level is negatively regulated by metabolic stress.

BMPER activates insulin signaling pathway through IR. To understand the underlying mechanism by which BMPER regulates insulin sensitivity and glucose tolerance, we focused on its impact on the canonical insulin signaling pathway that governs glucose output[27,28]. As expected, we observed BMPER

increased activation of insulin signaling pathway in the liver, skeletal muscle and heart, indicated by the phosphorylation of insulin receptor substrate1 (IRS1) and AKT (Fig. 3a). To determine whether BMPER regulates insulin signaling through modulating BMP signaling pathway, we used the BMPR2 kinase-dead (BMPR2-KD) mutant construct that inhibited BMP2-induced Smad 1, 5, 8 phosphorylation in primary hepatocytes (Supplementary Fig. 6a). However, BMPR2-KD mutant failed to inhibit BMPER-promoted IRS1 phosphorylation (Fig. 3b), suggesting BMPR2 is not required for the activation of IRS1 by BMPER. On the other hand, IRS1 phosphorylation induced by BMPER or insulin was blocked in IR-depleted hepatocytes isolated from IR-iKO mice (Fig. 3c). Thus, our data suggest that IR, but not BMP signaling, is required for BMPER activation of insulin signaling.

BMPER-activated insulin signaling requires NPC1 and BMPER internalization. To further understand how BMPER increased insulin signaling, we tested whether BMPER binds IR. However, we failed to observe the direct interaction of BMPER and recombinant IR, indicating BMPER regulates insulin pathway via unknown mediators. By performing co-immunoprecipitation-combined with liquid chromatography-mass spectrometry proteomic techniques, we identified NPC1, an endosome and lysosome-residing membrane protein[16], as an interacting protein of BMPER (Supplementary Fig. 6b, Table 2). NPC1 loss of function mutants develop devastating lysosomal cholesterol accumulation[29,30]. NPC1 also influences insulin signaling in adipocytes and NPC disease mouse models[31,32]. However, its exact role in insulin action remains unclear. Therefore, we tested the notion that NPC1 is required for BMPER to regulate insulin signaling. We confirmed NPC1 and BMPER were in the same complex and BMPER co-localized with endogenous NPC1 mainly in vesicles inside of hepatocytes (Fig. 4a-b). In addition, NPC1 knockdown markedly blocked BMPER, but not insulin, induced IRS1 phosphorylation (Fig. 4c-d), suggesting NPC1 specifically mediates BMPER-promoted insulin signaling. By performing immunoprecipitation studies with membrane fractions purified from hepatocytes, we discovered that BMPER was associated with endogenous IR *in vivo* and NPC1 knockdown markedly blocked the

BMPER and IR complex formation in hepatocytes (Fig. 3e, Supplementary Fig. 6c). These observations suggest NPC1 is required for BMPER to interact with IR and promote insulin signaling. Our previous studies demonstrate BMPER can be internalized into endothelial cells[15]. In hepatocytes, BMPER was also internalized and the internalized BMPER was degraded with a half-life at 38.45 min during a chase period with cold media (Supplementary Fig. 6d). Its internalization was inhibited by chlorpromazine (CPM), an inhibitor of clathrin-dependent endocytosis but not by methyl-β-cyclodextrin (MCD), an inhibitor of the caveolin-dependent endocytosis (Fig. 3f-g). In addition, CPM abolished IRS1 phosphorylation induced by BMPER (Fig. 3h, Supplementary Fig. 6e), suggesting BMPER internalization is required for IRS1 activation.

BMPER supplementation improves glucose homeostasis in diabetic mice. Since BMPER depletion resulted in defective glucose metabolism, we hypothesized that BMPER supplementation improves glucose homeostasis in diabetic mice. We injected adeno-associated virus (AAV) of BMPER, or AAV-GFP as the control, into mice and then fed them with HFD for eight weeks. We observed AAV-BMPER injection recovered BMPER plasma level in HFD-fed mice back to the level seen in control chow-fed mice (Fig. 5a) and had no impacts on appetite and weight gain (Supplementary Fig. 7a-b). However, plasma insulin and glucose levels were decreased in AAV-BMPER-injected mice compared to AAV-GFP group (Fig. 5b-c, Supplementary Fig. 7c-d). Moreover, responses of glucose clearance and insulin sensitivity were improved in AAV-BMPER- injected mice following HFD feeding, although no difference was observed in CC-fed mice (Fig. 5d, Supplementary Fig. 7e-f).

We also tested whether BMPER alleviates insulin resistance in a $Lepr^{db/db}$ (*db/db)* monogenic mouse model of severe diabetes. BMPER plasma level was markedly lower than wild-type (C57BL/6) mice and AAV-BMPER injection recovered BMPER level in *db/db* mice (Fig. 5e). We observed no differences in food intake and body weight between AAV-BMPER and AAV-GFP- injected mice (Supplementary Fig. 8a-b). However, AAV-BMPER injection led to the normalization of

hyperinsulinemia and hyperglycemia (Fig. 5f-g, Supplementary Fig. 8c-d) and improved glucose clearance and insulin sensitivity in *db/db* mice (Fig. 5h). Polyuria and glucosuria are important hallmark clinical features of T2DM. We observed dramatic decreases in urinary glucose and albumin levels and urine volume in AAV-BMPER- injected *db/db* mice (Fig. 5i-k).

The liver-specific IR knockout mice display severe insulin resistance and defects in insulin clearance[33]. Our signaling studies suggest that IR is required for BMPER-promoted insulin signaling (Fig. 3c). Therefore, we tested whether AAV-BMPER could improve glucose response in IR-iKO mice that developed insulin resistance and glucose intolerance (Fig. 5l). Although AAV-BMPER improved glucose response in diet-induced obese (DIO) and *db/db* mice (Fig. 5a-k), it failed to improve insulin resistance or glucose clearance in IR-iKO mice (Fig. 5l). It suggests that BMPER protects glucose homeostasis through an IR-dependent mechanism.

We also tested the feasibility of delivering recombinant BMPER protein *in vivo*. Following the injection of recombinant BMPER into HFD-fed mice, we detected significant normalization of hyperinsulinemia and improved glucose and insulin tolerance responses (Fig. 6). Taken together, our results suggest BMPER supplementation through AAV or recombinant protein delivery can improve T2DM.

Discussion

Taken together, our data unravel an unexpected role for BMPER in glucose homeostasis and indicate BMPER supplementation (i.e. gene therapy or recombinant protein delivery) can be a potential approach to treat T2DM and insulin resistance. Notably, the requirement of NPC1 and endocytosis for BMPER's action suggests a new perspective for transactivating insulin signaling. Although the exact role for NPC1 in BMPER IR complex formation and downstream insulin signaling events remains to be further characterized, our data strongly support that NPC1 can directly impact insulin signaling pathway through recruiting BMPER to IR.

The endothelium, by virtue of its location, tightly controls metabolic exchange between the circulation and surrounding tissues. Endothelial dysfunction and inflammation have been observed during the development of T2DM and insulin resistance[6,7], however, it remains a question how important endothelial cells are in the maintenance of metabolic homeostasis and how its dysregulation contributes to metabolic dyshomeostasis. Here, our data indicate BMPER is downregulated in humans with metabolic syndrome and DIO mice (Fig. 2), suggesting endothelial secretory function might also be disrupted during metabolic stress conditions and contribute to the progression of T2DM and insulin resistance.

Methods

Reagents and antibodies

All the chemicals and antibodies are listed in the main reagent table (Supplementary Table 3).

Mice

BMPER$^{flox;flox}$ mice were generated with standard CRISPR-cas9 gene editing technique. C57BL/6 embryos were microinjected with Cas9 protein, each guided RNA and a circular donor vector. Designed guide RNAs targeted intron 3 and intron 4 of the *bmper* gene for insertion of loxP sites flanking Exon 4 (Fig. 1a). Guide RNAs were evaluated in vitro using purified Cas9 and PCR-amplified target region. Functional guide RNAs were identified and used for model generation. Two founder animals were identified by specific PCR assays as positive for both 5' and 3' loxP site insertions. PCR assays spanning each loxP site followed by sequencing was also performed to confirm the loxP sequences. Spanning PCR assays across both loxP sites was performed to confirm *cis* orientation. Further validation to rule out random integration of the donor vector was performed, including long PCR assays across 5'

and 3' homology arms and PCR assays specific to the donor vector backbone. In addition, off-target analysis was performed on the original founders and no hits in any of the potential off-target sites screened were identified. Male chimeras were mated to wild-type C57BL/6 females to establish an isogenic line, and then backcrossed to C57BL/6 mice to obtain BMPER$^{flox/flox}$ mice on C57BL/6 background. All experiments were conducted on the resulting C57BL/6 background. Genomic DNA of BMPER$^{flox;flox}$ mice was isolated as described previously[12] and subjected for standard PCR assays to identify wild-type and targeted alleles. A PCR assay has been developed to genotype the pups. PCR samples were denatured in 95°C for 2 min, and then subjected to 35 cycles of three-step amplification, a 30-s 94°C denaturation, 30-s 50°C annealing, and 1-min 72°C extension step. A 740-bp product represents the wild-type allele and an 820-bp product (primers BMPER-SeqF and BMPER-SeqR) indicates the target allele. PCR primers: BMPER-SeqF, 5'- CGCACCCTCTAA CCTGTTCAGAC-3'; BMPER-SeqR, 5 _AGAACCACTGTTTTGCTCCAAGC-3'. The B6.Cg-Tg (CAG-cre/Esr1*) 5Amc/J (CAG-CreER$^{+/-}$) mice were obtained from Jackson Laboratories. The Cdh5 (PAC)-CreERT2 (Cdh5-CreER$^{+/-}$) mice were generously provided by Dr. Ralf H. Adams[34]. All mice were housed on a 12-hour light/dark cycle, with food and water *ad libitum*. All experimental procedures on mice were performed according to the National Institutes of Health Guide for the Care and Use of Laboratory Animals and approved by the Institutional Committee for the Use of Animals in Research at Baylor College of Medicine.

We used the mating of BMPER$^{flox;flox}$ and CAG-CreER$^{+/-}$ or BMPER$^{flox;flox}$ and Cdh5-CreER$^{+/-}$ mice to generate the BMPER$^{flox;flox}$; CAG-CreER$^{+/-}$ (WT or iKO) mice or BMPER$^{flox;flox}$; Cdh5-CreER$^{+/-}$ (eWT or eKO) male mice for control chow (CC, 14.7% calories from fat) or high-fat diet (HFD, 60% calories from fat)- induced diabetes studies. In addition, IR-iKO and their littermate control IR-WT mice were generated from the mating of IR$^{flox/flox}$ and CAG-CreER$^{+/-}$ mice followed by tamoxifen injection. Blood serum was obtained before and after they were fed with different diets. Primary hepatocytes were

isolated from 5~8 weeks mice. For insulin signaling experiments, mice were injected with insulin at 0.5 U/kg (for CC fed mice) or 1.0 U/kg (for HFD and *db/db* mice) and blood glucose levels were monitored. For adeno-associated virus (AAV)-transduced experiments, C57BL/6 and *db/db* mice at five weeks old were injected intravenously with the AAV-GFP or AAV-BMPER respectively at the titer at ~10^{12} per 25 g mice. C57BL/6 mice were then fed CC or HFD and *db/db* mice were fed CC as indicated. Metabolic studies were performed with these mice and tissues and serum were collected for further analysis.

Subjects

Plasma samples were obtained from the study[25] that was approved by the Institutional Review Board of Baylor College of Medicine. Male and female volunteers were recruited at the Center for Cardiometabolic Disease Prevention at Baylor College of Medicine, Houston, Texas, or by advertisement.

Cell lines and primary cells

HEK293 cells were grown in DMEM supplemented with 10% FBS and antibiotics (100 U/ml penicillin, 68.6 mol/L streptomycin). Primary hepatocytes were isolated using collagenase perfusion method from C57BL/6 mice based on previously published paper with modifications[35]. Briefly, the liver from 5 ~8 weeks old mice was perfused through the inferior vena cava with 7 ml pre-warmed (37°C) liver perfusion medium at 1 ml/min. Then, the liver was constantly digested with 5 ml pre-warmed (37°C) collagenase (1mg/ml) at 1 ml/min. The perfused liver was chopped gently in DMEM and centrifuged at 72 g for 2 minutes. Cells were washed with 20 ml hepatocyte wash medium and purified with 20 ml 45% (v/v) Percoll solution at 72 g for 2 min. Cell viability and number were measured through Trypan blue exclusion and manual counting. Hepatocytes were cultured in William's E medium containing 5% FBS, 100 units/ ml of penicillin and streptomycin, and primary hepatocyte maintenance supplements at 37°C in a 5% CO_2 incubator. For NPC1 depleted cells, primary hepatocytes were transduced with

lentiviral *NPC1* shRNA or control virus for 3 days. For signaling experiment, hepatocytes were starved overnight and treated with insulin at 100 nM and BMPER at 100 nM for 1 hour in all the experiments.

Analysis of endocrine hormones and metabolites

For fasting blood serum, mice were fasted 4 hours or overnight and then blood was collected through submandibular bleeding using a lancet. Plasma and urinary values for glucose were measured with a mouse endocrine multiplex assay, and insulin and albumin with ELISA kits.

Glucose/ insulin tolerance tests

Glucose tolerance tests (GTTs) and Insulin tolerance tests (ITTs) were performed following our established protocol[36]. Briefly, GTTs were performed after an overnight (for CC and HFD-fed mice or *db/db* mice) fasting. Blood glucose was measured before and 15, 30, 60, 120 min after an *i.p.* glucose injection (1 g/kg) with a Freestyle Glucose Monitoring System (Abbott Laboratories). ITTs were performed after 4 hours fasting. Blood glucose was measured before and indicated time periods after an *i.p.* insulin injection.

Hyperinsulinemic-euglycemic clamp studies

The hyperinsulinemic-euglycemic clamp studies were performed in unrestrained mice using the insulin clamp technique (with constant insulin dose) in combination with [^{3}H] glucose and [^{14}C]2-deoxyglucose following our established protocol. In summary, mice were cannulated as described previously[37] and allowed to recover for 4 to 7 days before the clamp. After an overnight fasting, mice received a primed dose of [^{3}H]glucose (10 μCi) and then a constant rate intravenous infusion (0.1 μCi/min) of [^{3}H]glucose using a syringe infusion pump for 90 minutes. Blood samples were collected for the determination of basal glucose production. After 90 minutes, mice were primed with a bolus injection of insulin followed by a 2-hour continuous insulin infusion. Simultaneously, 25% glucose was infused at an adjusted rate to

maintain the blood glucose level at 100-140 mg/dl. Blood glucose concentration was determined every 10 minutes by a glucometer. At the end of a 120-minute period, blood was collected for the measurements of hepatic glucose production and peripheral glucose disposal rates. For tissue specific uptake, we inject 2-deoxy-D-[1,-^{14}C] glucose (10 μCi) into bolus during hyperinsulinemic-euglycemic clamp at 45 min before the end of the clamps and collect blood sample at 5, 10, 15, 25, 35 and 45 minutes. At the end of the clamp, mouse tissues were harvested for the evaluation of glucose uptake. Glucose uptake in different tissues was calculated from plasma 2-[^{14}C] deoxyglucose profile and tissue content of [^{14}C] glucose-6 phosphate.

Indirect calorimetry and metabolic cage studies

This assay was performed following our established protocol[36] with minor modification. Mice were individually housed in metabolic chambers maintained at 20–22ºC on a 12-h light/dark cycle. Metabolic measurements (oxygen consumption, food and water intake, locomotor activity) were recorded using an Oxymax/CLAMS (Columbus Instruments) open-circuit indirect calorimetry system. Food and water intake were also monitored. To determine the amount of urinary albumin excretion, individual mice were separated in a metabolic cage, where urine was collected and measured for 24 h. The urinary volume and its glucose and albumin concentration was determined.

Membrane fractionation

Membrane fractionation was performed following our published protocol with small modification[15]. Briefly, tissue or cells were washed twice with cold PBS and suspended in buffer A (10 mM HEPES, pH 7.9; 10 mM KCl; 0.1 mM EDTA, 1 mM DTT, protease inhibitor). The mixture was homogenized and incubated on ice for 10 min, and then centrifuged at 4°C at 10,000 g for 3 min. The supernatant was collected and further centrifuged at 100,000 g at 4 °C for 1 hour. The cloudy pellet was washed and dissolved in the lysis buffer as the membrane fraction, which was used for further analysis.

Immunoblotting and immunoprecipitation

Immunoblotting experiments were performed based on our previously published paper[38]. Briefly, cells were harvested in lysis buffer (1% Triton X-100, 50 mM Tris, pH 7.4, 150 mM NaCl, 10% glycerol and protease and phosphatase inhibitors) and clarified by centrifugation at 8000 g for 5 min. Equal amounts of protein were loaded on the SDS-PAGE gel and subjected for Western blotting. For endogenous immunoprecipitation (IP) experiments, protein A/G Plus-agarose was used to pull down antibody complexes following our established methods[13]. For transient transfection, HEK293 cells were transfected with Flag-tagged NPC1, GFP-tagged BMPER plasmid or both together with Lipofectamine 2000. Two days later, cell lysates were harvested and IPed with anti-Flag resin and precipitates were blotted with anti-GFP and anti-flag antibodies. For endogenous IP, primary hepatocytes were transduced with lentiviral control or NPC1 shRNA, respectively. 3 days later, purified flag-tagged BMPER protein was added to the medium for 30 min. Cells were then washed with cold PBS and cross-linked with DSP at 4°C for 2 hours. Cells were harvested and membrane fractions were used for IP experiments.

Gene expression analysis (real-time PCR)

Total RNAs were reversely transcribed into cDNAs with iScript™ cDNA synthesis kit. The specific pairs of primers used for the real-time PCR are listed in Supplementary Table 4 (designed by Universal ProbeLibrary Assay Design Center tool from Roche, Indianapolis, IN). The real-time PCR was performed with FastStart Universal Probe Master mix, specific primers and probes for each gene (Universal ProbeLibrary Probes #19 for G6Pase, #49 for PEPCK, #58 for GK, #77 for SREBP1, #38 for IL1β, #6 for IL6, #25 for TNFα, #64 for β-Actin, #79 for BMPER, #20 for BMP2, #63 for BMP4, #22 for BMP6, #1 for BMP7, #38 for BMP9, #67 for BMPR2) in Roche Lightcycler 480 PCR machine. Reaction mixtures were incubated at 95°C for 10 min followed by 55 cycles at 95°C for 10 sec and 60°C for 30 sec. β-Actin was used as the housekeeping gene.

Quantification and statistical analysis

No statistical methods were used to predetermine the sample size. No randomization was used as all mice used were genetically defined, inbred mice. Statistical data were drawn from normally distributed group with similar variance between groups. Data are shown as the mean ± SEM. Differences were analyzed with Student's *t*-test, 1-way or 2-way ANOVA and followed by a Fisher's LSD test unless otherwise specifically stated. Values of $P \leq 0.05$ were considered statistically significant.

Acknowledgements

We would like to thank the MMPC Core at BCM and NIH fund RO1DK114356 & UM1HG006348 for core services.

Sources of funding

This study was supported by grants from the US National Institutes of Health (NIH): R01HL122736 (to L.X.), R01HL112890 and HL061656 (to X.P.). This work was also funded by and American Diabetes Association #1-18-IBS-105 (to S.M.H).

DISCLOSURES

None.

REFERENCES

1. Caspard, H., *et al.* Recent trends in the prevalence of type 2 diabetes and the association with abdominal obesity lead to growing health disparities in the USA: An analysis of the NHANES surveys from 1999 to 2014. *Diabetes Obes Metab* **20**, 667-671 (2018).
2. Cho, N.H., *et al.* IDF Diabetes Atlas: Global estimates of diabetes prevalence for 2017 and projections for 2045. *Diabetes Res Clin Pract* **138**, 271-281 (2018).
3. Chawla, A., Nguyen, K.D. & Goh, Y.P. Macrophage-mediated inflammation in metabolic disease. *Nat Rev Immunol* **11**, 738-749 (2011).
4. Xu, H., *et al.* Chronic inflammation in fat plays a crucial role in the development of obesity-related insulin resistance. *J Clin Invest* **112**, 1821-1830 (2003).
5. Pober, J.S. & Sessa, W.C. Evolving functions of endothelial cells in inflammation. *Nat Rev Immunol* **7**, 803-815 (2007).
6. De Vriese, A.S., Verbeuren, T.J., Van de Voorde, J., Lameire, N.H. & Vanhoutte, P.M. Endothelial dysfunction in diabetes. *Br J Pharmacol* **130**, 963-974 (2000).
7. van den Oever, I.A., Raterman, H.G., Nurmohamed, M.T. & Simsek, S. Endothelial dysfunction, inflammation, and apoptosis in diabetes mellitus. *Mediators Inflamm* **2010**, 792393 (2010).
8. Goumans, M.J., Zwijsen, A., Ten Dijke, P. & Bailly, S. Bone morphogenetic proteins in vascular homeostasis and disease. *Cold Spring Harb Perspect Biol* **10**(2018).
9. Moser, M., *et al.* BMPER, a novel endothelial cell precursor-derived protein, antagonizes bone morphogenetic protein signaling and endothelial cell differentiation. *Mol Cell Biol* **23**, 5664-5679 (2003).
10. Dyer, L., *et al.* BMPER promotes epithelial-mesenchymal transition in the developing cardiac cushions. *PLoS One* **10**, e0139209 (2015).
11. Dyer, L., Pi, X. & Patterson, C. Connecting the coronaries: how the coronary plexus develops and is functionalized. *Dev Biol* **395**, 111-119 (2014).
12. Kelley, R., *et al.* A concentration-dependent endocytic trap and sink mechanism converts Bmper from an activator to an inhibitor of Bmp signaling. *J Cell Biol* **184**, 597-609 (2009).
13. Lockyer, P., *et al.* LRP1-dependent BMPER signaling regulates lipopolysaccharide-induced vascular inflammation. *Arterioscler Thromb Vasc Biol* **37**, 1524-1535 (2017).
14. Pi, X., *et al.* Bmper inhibits endothelial expression of inflammatory adhesion molecules and protects against atherosclerosis. *Arterioscler Thromb Vasc Biol* **32**, 2214-2222 (2012).
15. Pi, X., *et al.* LRP1-dependent endocytic mechanism governs the signaling output of the bmp system in endothelial cells and in angiogenesis. *Circ Res* **111**, 564-574 (2012).
16. Higgins, M.E., Davies, J.P., Chen, F.W. & Ioannou, Y.A. Niemann-Pick C1 is a late endosome-resident protein that transiently associates with lysosomes and the trans-Golgi network. *Mol Genet Metab* **68**, 1-13 (1999).
17. Kwon, H.J., *et al.* Structure of N-terminal domain of NPC1 reveals distinct subdomains for binding and transfer of cholesterol. *Cell* **137**, 1213-1224 (2009).
18. Poisson, J., *et al.* Liver sinusoidal endothelial cells: Physiology and role in liver diseases. *J Hepatol* **66**, 212-227 (2017).
19. Li, M., Qian, M. & Xu, J. Vascular endothelial regulation of obesity-associated insulin resistance. *Front Cardiovasc Med* **4**, 51 (2017).
20. Pi, X., Xie, L. & Patterson, C. Emerging roles of vascular endothelium in metabolic homeostasis. *Circ Res* **123**, 477-494 (2018).
21. Elsen, M., *et al.* BMP4 and BMP7 induce the white-to-brown transition of primary human adipose stem cells. *Am J Physiol Cell Physiol* **306**, C431-440 (2014).

22. Guiu-Jurado, E.*, et al.* Bone morphogenetic protein 2 (BMP2) may contribute to partition of energy storage into visceral and subcutaneous fat depots. *Obesity (Silver Spring)* **24**, 2092-2100 (2016).
23. Hata, K.*, et al.* Differential roles of Smad1 and p38 kinase in regulation of peroxisome proliferator-activating receptor gamma during bone morphogenetic protein 2-induced adipogenesis. *Mol Biol Cell* **14**, 545-555 (2003).
24. Schleinitz, D.*, et al.* Genetic and evolutionary analyses of the human bone morphogenetic protein receptor 2 (BMPR2) in the pathophysiology of obesity. *PLoS One* **6**, e16155 (2011).
25. Khan, I.M.*, et al.* Postprandial monocyte activation in individuals with metabolic syndrome. *J Clin Endocrinol Metab* **101**, 4195-4204 (2016).
26. Alberti, K.G.*, et al.* Harmonizing the metabolic syndrome: a joint interim statement of the International Diabetes Federation Task Force on Epidemiology and Prevention; National Heart, Lung, and Blood Institute; American Heart Association; World Heart Federation; International Atherosclerosis Society; and International Association for the Study of Obesity. *Circulation* **120**, 1640-1645 (2009).
27. Taniguchi, C.M., Emanuelli, B. & Kahn, C.R. Critical nodes in signalling pathways: insights into insulin action. *Nat Rev Mol Cell Biol* **7**, 85-96 (2006).
28. Boucher, J., Kleinridders, A. & Kahn, C.R. Insulin receptor signaling in normal and insulin-resistant states. *Cold Spring Harb Perspect Biol* **6**(2014).
29. Carstea, E.D.*, et al.* Niemann-Pick C1 disease gene: homology to mediators of cholesterol homeostasis. *Science* **277**, 228-231 (1997).
30. Loftus, S.K.*, et al.* Murine model of Niemann-Pick C disease: mutation in a cholesterol homeostasis gene. *Science* **277**, 232-235 (1997).
31. Fletcher, R.*, et al.* The role of the Niemann-Pick disease, type C1 protein in adipocyte insulin action. *PLoS One* **9**, e95598 (2014).
32. Ong, Q.R., Lim, M.L., Chua, C.C., Cheung, N.S. & Wong, B.S. Impaired insulin signaling in an animal model of Niemann-Pick Type C disease. *Biochem Biophys Res Commun* **424**, 482-487 (2012).
33. Michael, M.D.*, et al.* Loss of insulin signaling in hepatocytes leads to severe insulin resistance and progressive hepatic dysfunction. *Mol Cell* **6**, 87-97 (2000).
34. Wang, Y.*, et al.* Ephrin-B2 controls VEGF-induced angiogenesis and lymphangiogenesis. *Nature* **465**, 483-486 (2010).
35. Li, W.C., Ralphs, K.L. & Tosh, D. Isolation and culture of adult mouse hepatocytes. *Methods Mol Biol* **633**, 185-196 (2010).
36. Mao, H.*, et al.* Endothelial LRP1 regulates metabolic responses by acting as a co-activator of PPARgamma. *Nat Commun* **8**, 14960 (2017).
37. Louet, J.F.*, et al.* The coactivator SRC-1 is an essential coordinator of hepatic glucose production. *Cell Metab* **12**, 606-618 (2010).
38. Mao, H., Lockyer, P., Townley-Tilson, W.H., Xie, L. & Pi, X. LRP1 regulates retinal angiogenesis by inhibiting PARP-1 activity and endothelial cell proliferation. *Arterioscler Thromb Vasc Biol* **36**, 350-360 (2016).

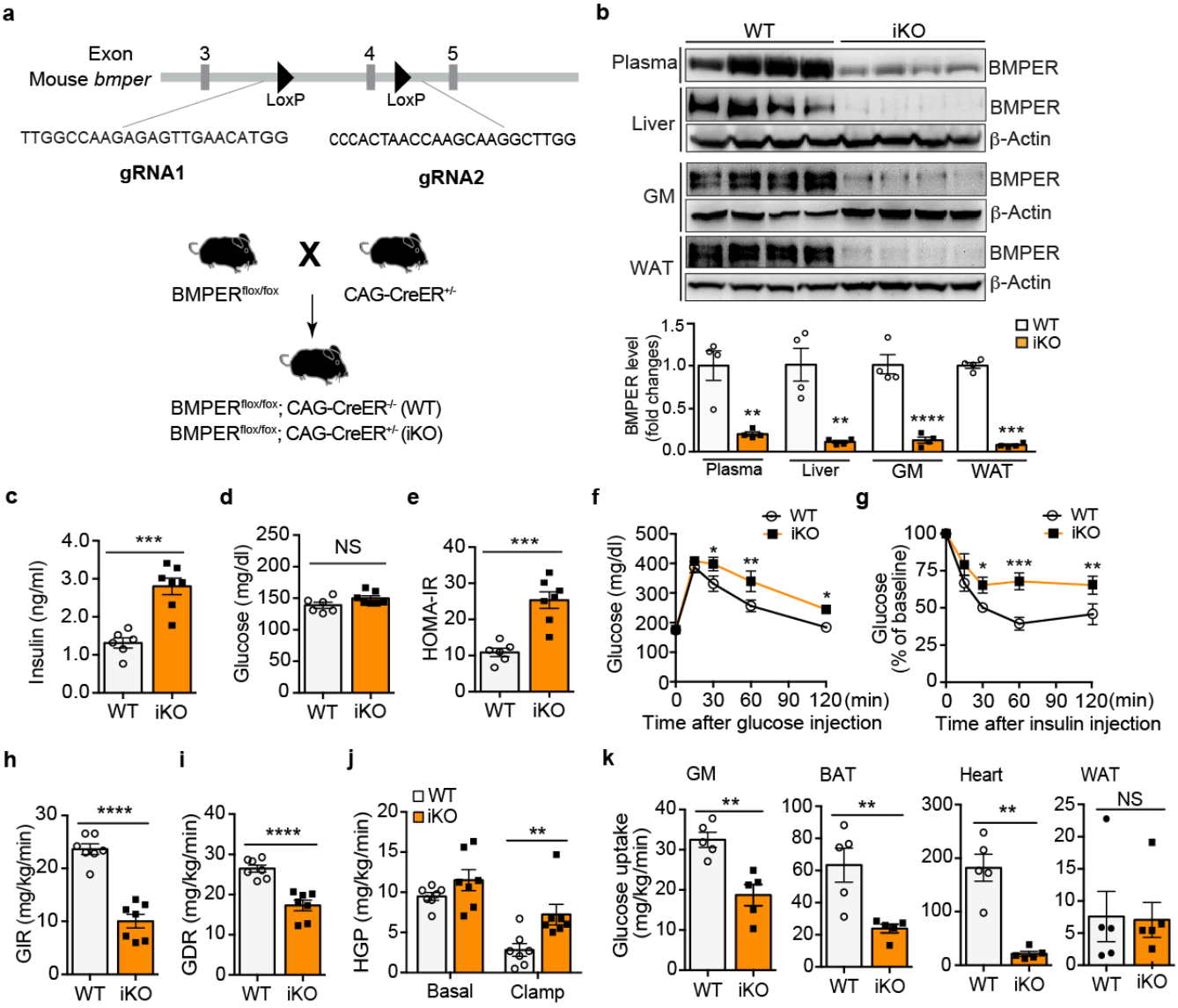

Figure 1. BMPER depletion causes mice to develop hyperinsulinemia, glucose intolerance and insulin resistance. (**a)** The generation of the BMPER iKO mouse model. The gRNA-guided CRISPR/Cas9 strategy was used for targeted deletion of *bmper* gene. (**b**) BMPER depletion was examined with Western blotting. (**c-e**) Fasted insulin and glucose, HOMA-IR. (**f-g**) Glucose and insulin tolerance tests. (**h**) Glucose infusion rate (GIR). (**i**) Glucose disposal rate (GDR). (**j-k**) Hepatic glucose production (HGP; **j**) and glucose uptake in peripheral tissues (**k**) were analyzed with hyperinsulinemic-euglycemic clamps. GM, gastrocnemius muscle; BAT, brown adipose tissue; WAT, white adipose tissue.

WT, BMPER$^{flox/flox}$; CAG-CreER$^{-/-}$. iKO, BMPER$^{flox/flox}$; CAG-CreER$^{+/-}$. n=4 (**b**), 8 (**c-g**) and 7 (**h-k**). *, $P< 0.05$. **, $P< 0.01$. ***, $P< 0.001$. ****, $P< 0.0001$. NS, not significant.

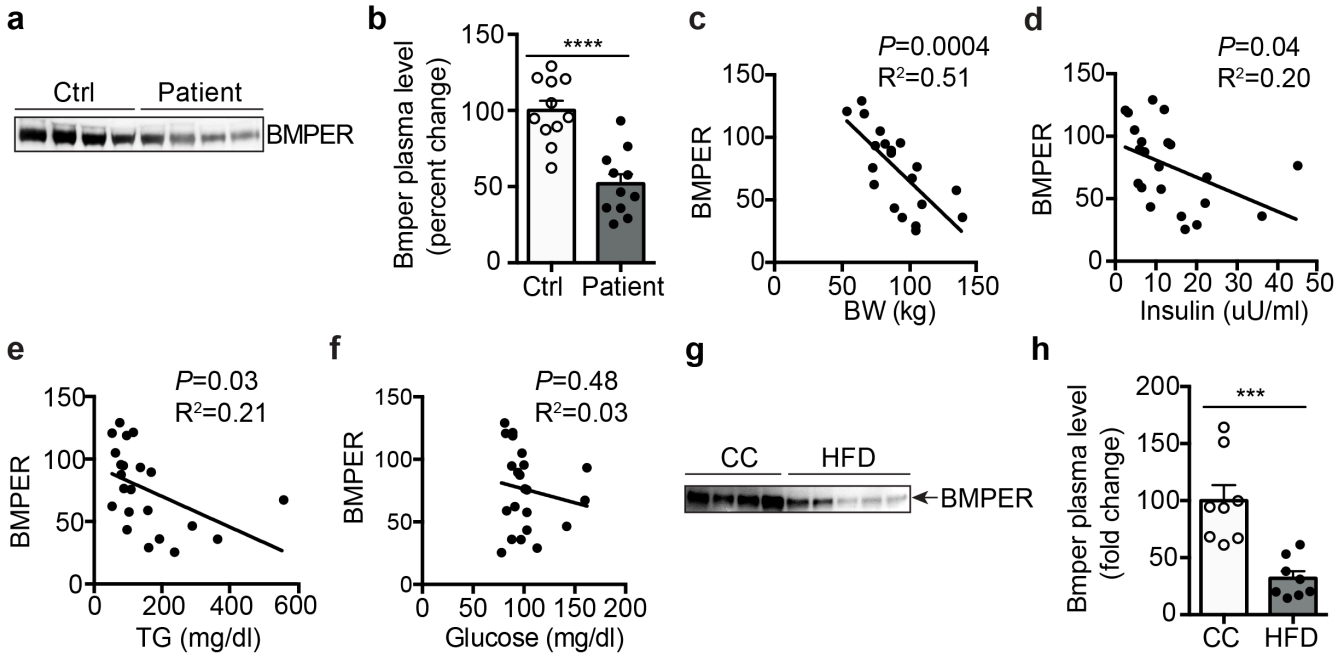

Figure 2. BMPER plasma level decreases in metabolic syndrome patients and DIO mice. (**a-b**) BMPER plasma levels were decreased in metabolic syndrome (MS) patients[25]. (**c-f**) BMPER plasma level was associated with body weight (BW), insulin and triglyceride (TG) plasma levels in MS patients. Correlation was computed for Pearson correlation coefficients with an assumption of Gaussian distribution. (**g-h**) BMPER plasma level was decreased in HFD-fed mice. n=11 (**b-f**) and 8 (**h**). ***, $P< 0.001$. ****, $P< 0.0001$.

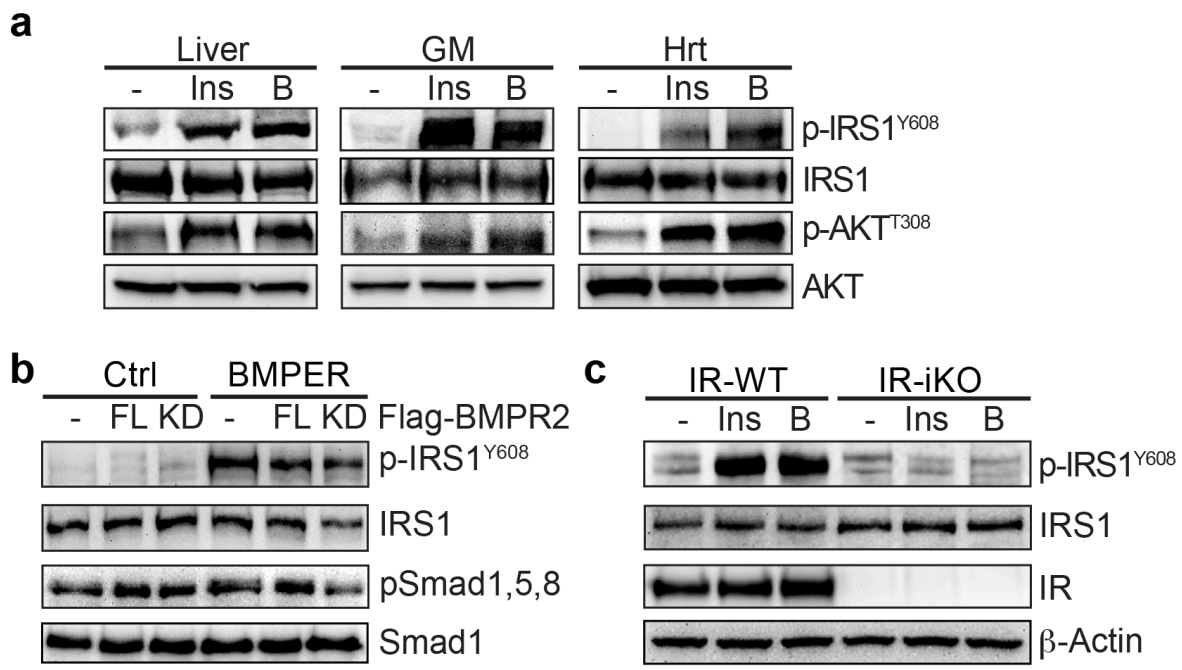

Figure 3. BMPER promotes insulin signaling through IR but not BMPR2. (**a**) BMPER (B, 1 hour) or insulin (Ins, 0.5 hour) was injected (*i.p.*) into mice. Tissues, including liver, GM (gastrocnemius muscle) and Hrt (heart), were used for Western blotting. (**b**) Hepatocytes were transduced with adenovirus of flag-tagged BMPR2 full-length (FL) or kinase-dead mutant (KD). Cells were then treated with BMPER (1 hr) and harvested for Western blotting. (**c**) Hepatocytes were isolated from IR-iKO and their littermate control (IR-WT) mice. Cells were treated with insulin (Ins, 0.5 hour) or BMPER (B, 1 hour) and harvested for Western blotting. IR-WT, $IR^{flox/flox}$; CAG-$CreER^{-/-}$. IR-iKO, $IR^{flox/flox}$; CAG-$CreER^{+/-}$.

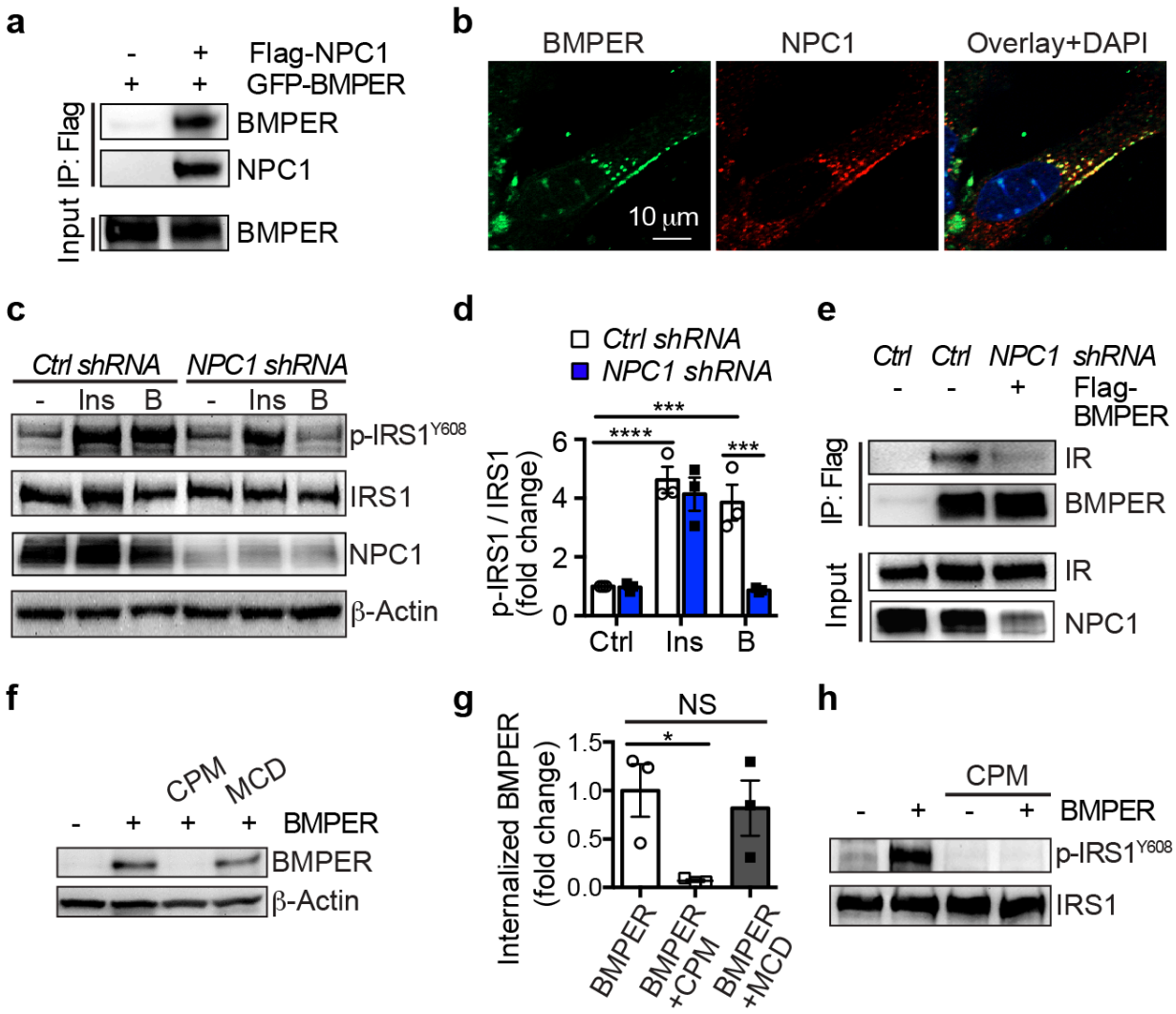

Figure 4. BMPER promotes insulin signaling through NPC1 and endocytosis. (**a**) Co-immunoprecipitation of GFP-tagged BMPER and flag-tagged NPC1 in HEK293 cells. (**b**) Hepatocytes were treated with flag-tagged BMPER for 30 min and staining of BMPER and endogenous NPC1 was performed. (**c-d**) Hepatocytes were transduced with *NPC1* shRNA lentivirus and then treated with flag-tagged BMPER (B, 1 hr) or insulin (Ins, 30 min). Western blotting was performed and band intensity was quantified (**d**). (**e**) Hepatocytes were transduced with *NPC1* shRNA lentivirus and then treated with flag-tagged BMPER (B, 1 hr). Membrane fractions were separated and then subjected for immunoprecipitation with flag antibody. (**f-g**) Hepatocytes were treated with chlorpromazine (CPM, 50 μM) or methyl-β-cyclodextrin (MCD, 10 mM). 30 minutes later, cells were pulsed with flag-BMPER (100 nM) for 1 hour and cell lysates were used for Western blotting. Internalized BMPER was

quantified in (**g**). (**h**) Hepatocytes were treated with CPM for 30 min, and then treated with BMPER for the detection of IRS1 phosphorylation. n=3 (**d, g**). *, $P< 0.05$. ***, $P< 0.001$. ****, $P< 0.0001$. NS, not significant.

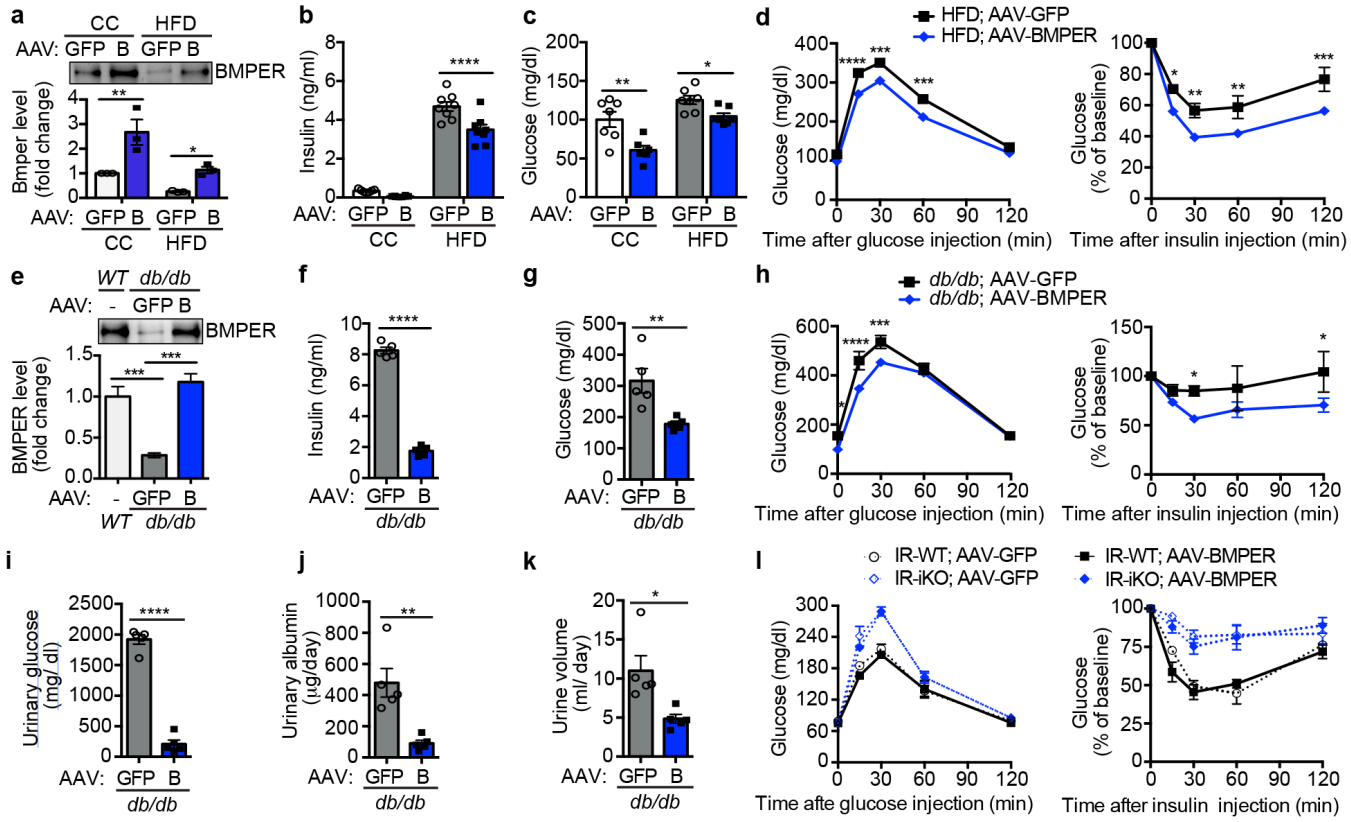

Figure 5. AAV-BMPER improves glucose responses in diabetic mice. (**a**) BMPER plasma levels in C57BL/6 (WT), AAV-GFP or AAV-BMPER (B)- injected mice that were fed HFD or CC diet. (**b-c**) Fasted insulin and glucose. (**d**) Glucose and insulin tolerance tests. (**e**) BMPER plasma levels in C57BL/6 (WT), AAV-GFP or AAV-BMPER (B)- injected *db/db* mice. (**f-g**) Fasted insulin and glucose. (**h**) Glucose and insulin tolerance tests. (**i**) Urinary glucose levels. (**j**) Urinary albumin levels. (**k**) Urine volume. (**l**) Glucose and insulin tolerance tests. IR-WT, $IR^{flox/flox}$; CAG-$CreER^{-/-}$. IR-iKO, $IR^{flox/flox}$; CAG-$CreER^{+/-}$. n=3 (**a**), 8 (**b-d**), 5 for the AAV-GFP and 7 for AAV-BMPER group (**e-k**) and 4 (**l**). *, $P< 0.05$. **, $P< 0.01$. ***, $P< 0.001$. ****, $P< 0.0001$.

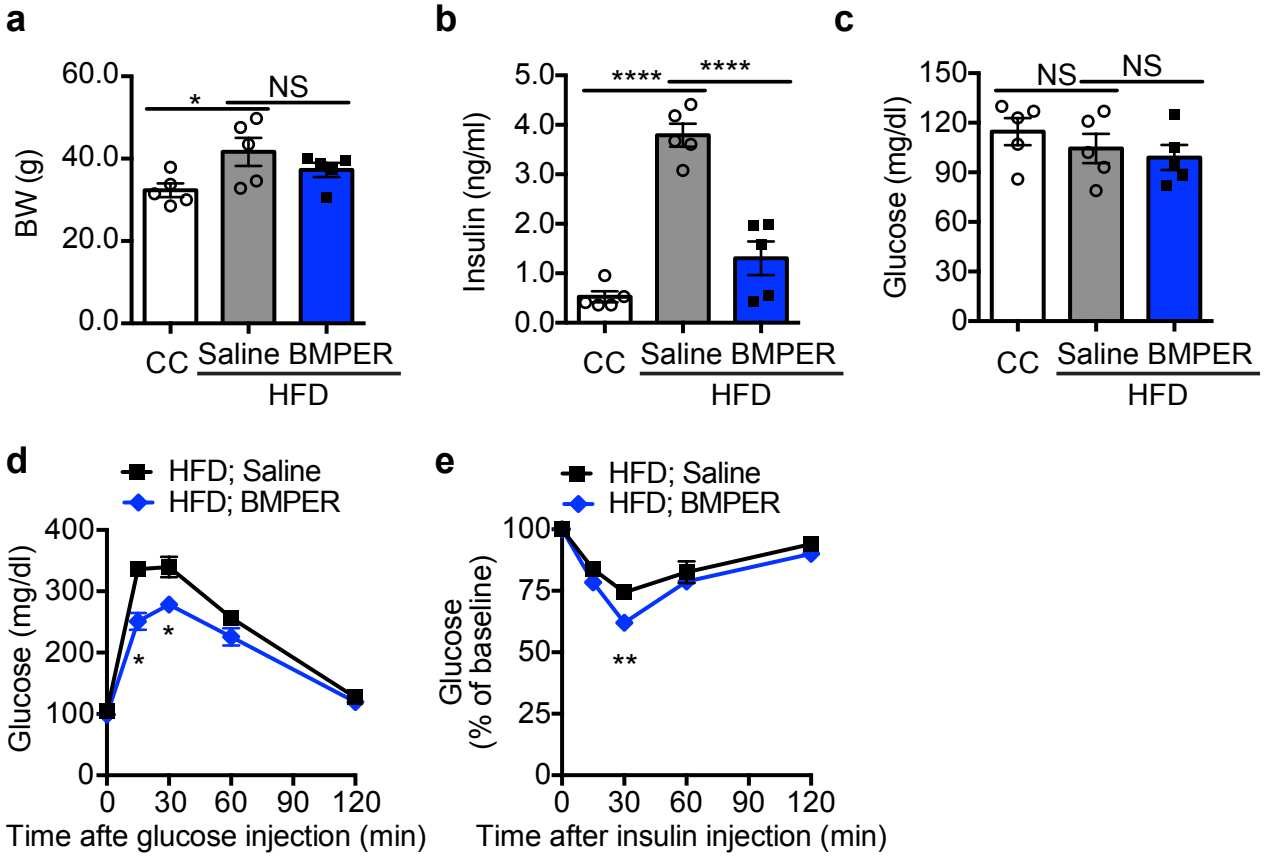

Figure 6. Recombinant BMPER protein improves glucose responses in DIO mice. C57BL/6 mice were fed HFD or control chow (CC) for 4 weeks and then injected with recombinant BMPER protein at 0.1 mg/kg/mouse every other day for 6 weeks. Metabolic parameters were measured, including (**a**) Body weight. (**b**) Fasted insulin. (**c**) Fasted glucose. (**d**) Glucose tolerance tests. (**e**) Insulin tolerance tests. n=5 for each group. *, $P< 0.05$. **, $P< 0.01$. ****, $P< 0.0001$. NS, not significant.

Supplementary Table 1. Metabolic parameters.

Parameters	WT	iKO
BW (g)	32.25 ± 0.86	32.18 ± 1.05$^{(NS)}$
Glucose (mg/dl)		
Fasted	139.0 ± 4.79	150.0 ± 3.81$^{(NS)}$
Fed	174.7 ± 6.12	176.4 ± 8.134$^{(NS)}$
Insulin (ng/ml)		
Fasted	1.31 ± 0.13	2.80 ± 0.22^{c}
Fed	2.81 ± 0.20	16.77 ± 0.42^{d}
TG (mg/dl)	73.12 ± 4.25	85.78 ± 3.30^{a}
FFA (mEq/I)	0.78 ± 0.10	0.78 ± 0.05$^{(NS)}$

NS, not significant.

^{a} P<0.05, ^{b} P<0.01, ^{c} P<0.001, ^{d} P<0.0001

WT, BMPER$^{flox/flox}$;CAG-CreER$^{-/-}$.

iKO, BMPER$^{flox/flox}$;CAG-CreER$^{+/-}$.

Supplementary Table 2. Mass spectrometry result shows representative proteins that potentially form complex with BMPER.

Gene ID	GeneSymbol	SRA	PSMs	iBAQ
3939	LDHA	S	118	0.38
4000	LMNA	S	100	0.17
8514	KCNAB2	S	49.2	0.12
4864	NPC1	S	19.2	0.05
54887	UHRF1BP1	S	13.5	0.02

S: high confidence; R: medium confidence; A: weak confidence

PSMs: total normalized peptide hits

iBAQ: total abundance of the gene

Supplementary Table 3. Main reagent table.

REAGENT or RESOURCE	SOURCE	IDENTIFIER
Antibodies		
LRP1-CTD	Sigma	Cat#L2170
BMPER (Crossveinless-2/CV-2)	R&D Systems	Cat# AF2299
NPC1	Abcam	Cat# 124801
IRS-1	Cell signaling	Cat#2382
phospho- IRS1 (Tyr612)	Millipore	Cat#09-432
Akt	Cell signaling	Cat#9272
phospho-Akt (Ser473)	Cell signaling	Cat#9271
phospho-Akt (Thr308) (D25E6)	Cell signaling	Cat#13038
Insulin Receptor β (4B8)	Cell signaling	Cat#3025
β-Actin (C4) -HRP	Santa Cruz	Cat#sc-47778
Smad1	Cell signaling	Cat#9743
phospho- Smad1/Smad5/Smad8 (Ser463/465)	EMD Millipore	Cat#AB3848-I
Flag antibody	Sigma-Aldrich	Cat#2426
EZview Red ANTI-FLAG M2 Affinity Gel	Sigma-Aldrich	Cat#F2426
Chemicals, Peptides, and Recombinant Proteins		
60% high-fat diet (HFD)	Research Diets	Cat#D12492
Insulin	Novolin R	Cat#0169-1833-11
Mouse BMPER (Crossveinless-2) Protein	R&D Systems	Cat#2299-CV-050
Protein A/G Plus-agarose beads	Santa Cruz	Cat#sc-2003
iScript™ cDNA synthesis kit	Bio-Rad Laboratories	Cat#1708891

iTaq SYBR Green supermix	Bio-Rad Laboratories	Cat#1725121
TaqMan™ Universal PCR Master Mix	Thermo Scientific	Cat#4304437
Insulin solution	Santa Cruz	Cat# 11061-68-0
Cell maintenance supplements	Gibco	Cat# A15564
Tamoxifen	Sigma-Aldrich	Cat#T5648
Lipofectamine 2000	Thermo Scientific	Cat#11668019
Perfusion Medium	Thermo Scientific	Cat#17701038
Collagenase	Sigma-Aldrich	Cat#C5168
DMEM	Thermo Scientific	Cat#11965118
William's E Medium	Thermo Scientific	Cat#12551-032
Immobilon-P transfer membrane	Millipore	IPVH00010
Wash Medium	Thermo Scientific	Cat#17704-024
Percoll	GE Healthcare	Cat#17089101
OptiPrep density gradient medium	Sigma-Aldrich	Cat#1556
Penicillin & Streptomycin	Thermo Scientific	Cat#15140122
Fetal bovine serum (FBS)	Sigma-Aldrich	Cat#F0926
Horse serum	Thermo Scientific	Cat#16050114
Maintenance supplements	Thermo Scientific	Cat#CM4000
Chlorpromazine (CPM)	Sigma-Aldrich	Cat#C8138
Methyl-β-cyclodextrin (MCD)	Sigma-Aldrich	Cat#M7439
Critical Commercial Assays		
Insulin ELISA kit	Millipore	Cat#EZRMI-13K
RNA purification kit	QIAGEN	Cat#74104
Infinity Glucose kit	Thermo Scientific	Cat#TR15421
Albumin ELISA kit	Abcam	Cat#ab108792

Experimental Models: Cell Lines		
Primary hepatocytes	This paper	N/A
HEK293 cells	ATCC	Cat#CRL-1573
Experimental Models: Organisms/Strains		
Mouse: B6.Cg-Tg (CAG-cre/ Esr1*) 5Amc/J (CAG-CreER$^{+/-}$)	Jackson Laboratories	JAX: 004682
Mouse: Cdh5(PAC)-CreERT2 (Cdh5-CreER$^{+/-}$)	Dr. Ralf H. Adams from Max Planck Institute for Molecular Biomedicine, Germany	N/A
Mouse: C57BL/6	Jackson Laboratories	JAX: 000664
Mouse: IR^{flox}	Jackson Laboratories	JAX: 006955
Mouse: B6 db	Jackson Laboratories	JAX: 000697
Recombinant DNA		
Npc1 mouse shRNA plasmid	Origene	Cat#TL501501
pCMV-Tag2 vector	Agilent	Cat#211172
Scrambled shRNA plasmid	OriGene	Cat#TR30021
pLenti-C-Flag-DDK-BMPER	This paper	N/A
Ad-CMV-iCre	Vector Biolabs	Cat#1045

Supplementary Table 4. Sequence information for qPCR primers.

Gene	Forward primer	Reverse primer
G6Pase	5'- tctgtcccggatctaccttg-3'	5'- gaaagtttcagccacagcaa-3'
PEPCK	5'- ggagtacccattgagggtatcat-3'	5'- gctgagggcttcatagacaag-3'
GK	5'- cagatgctggatgacagagc-3'	5'- gccaggatctgctctaccttt-3'
SREBP1	5'- acaagattgtggagctcaaagac-3'	5'- tgcgcaagacagcagattta-3'
IL1β	5'- agttgacggaccccaaaag-3'	5'- agctggatgctctcatcagg-3'
IL6	5'- gctaccaaactggatataatcagga-3'	5'- ccaggtagctatggtactccagaa-3'
TNFα	5'- ctgtagcccacgtcgtagc-3'	5'- ttgagatccatgccgttg-3'
β-Actin	5'- ccaaccgtgaaaagatgacc-3'	5'- accagaggcatacagggaca-3'
BMPER	5'- ggctgagccatgtgtcct-3'	5'- cgcacctcagactctgtcac-3'
BMP2	5'- agatctgtaccgcaggcact-3'	5'- gttcctccacggcttcttc-3'
BMP4	5'- gatctttaccggctccagtct-3'	5'- tgggatgttctccagatgttc-3'
BMP6	5'- actgactagcgcgcagga-3'	5'- tgtggggagaactccttgtc-3'
BMP7	5'- cgagaccttccagatcacagt-3'	5'- cagcaagaagaggtccgact-3'
BMP9	5'- ggaagctgtgggtagatgacc-3'	5'- caagtcggtggggatgat-3'
BMPR2	5'- gagccctcccttgacctg-3'	5'- gtatcgaccccgtccaatc-3'

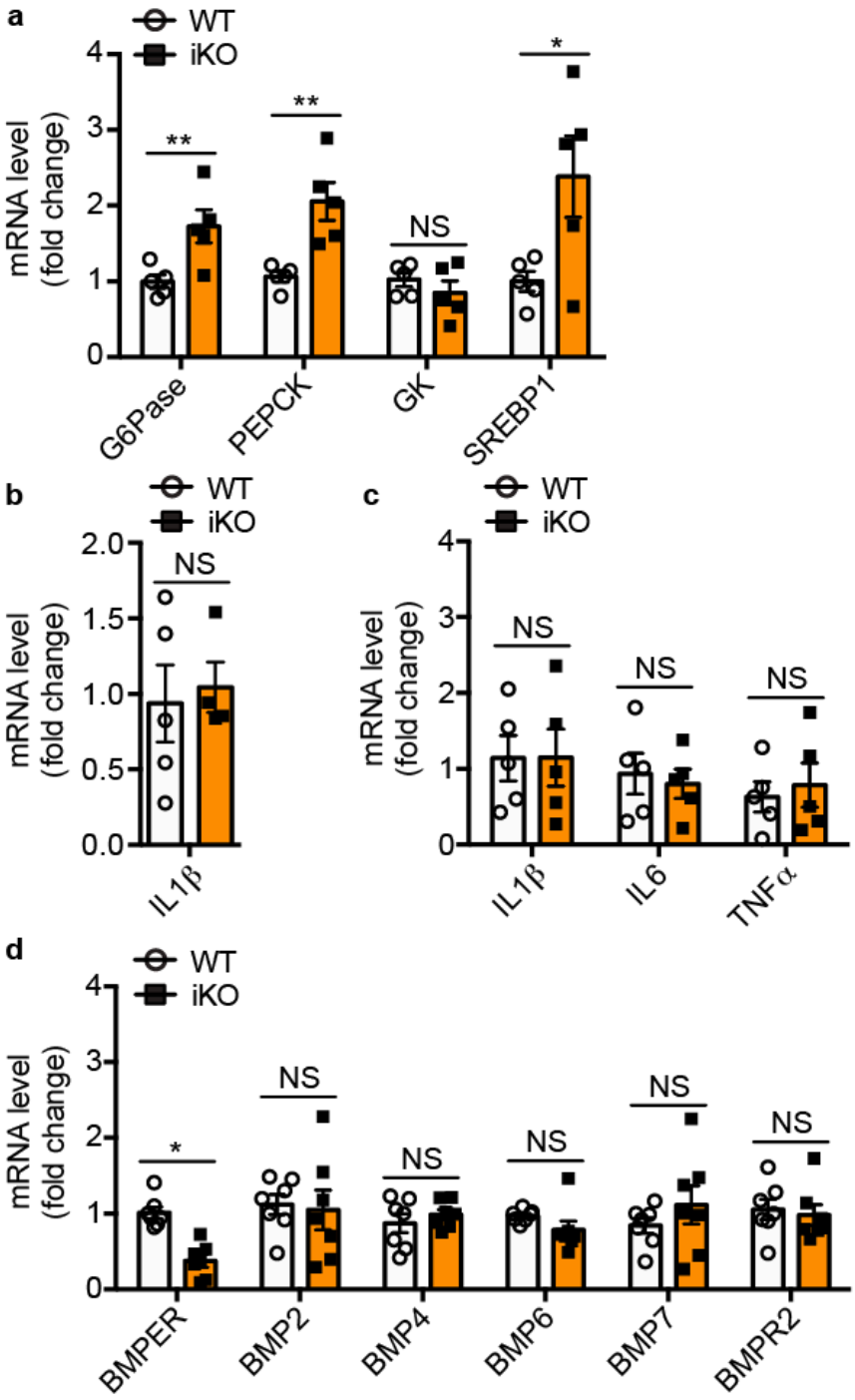

Supplementary Figure 1. Gene expression changes in liver and WAT tissues of BMPER iKO mice. (**a-d**) Real-time PCR assays were performed for indicated genes in the liver (**a, b, d**) and WAT (**c**) of BMPER iKO and their littermate control (WT) mice. n=5 (**a-c**) and 7 (**d**). *, $P< 0.05$. **, $P< 0.01$. NS, not significant.

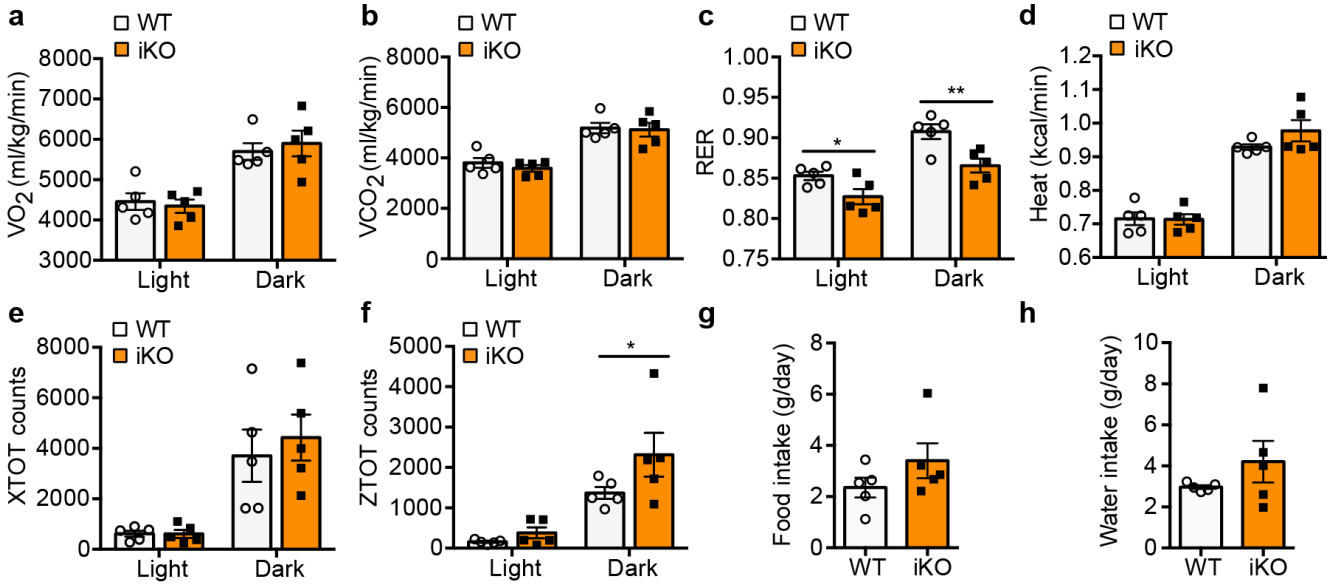

Supplementary Figure 2. CLAMS studies with BMPER iKO mice. Indirect calorimetry studies were performed to evaluate VO_2 (**a**), VCO_2 (**b**), respiratory exchange ratio (RER, **c**), heat (**d**), locomotor activity in x axis (XTOT, **e**) and z axis (ZTOT, **f**), daily food (**g**) and water intake (**h**). n=5 (**a-h**). *, $P< 0.05$. **, $P< 0.01$.

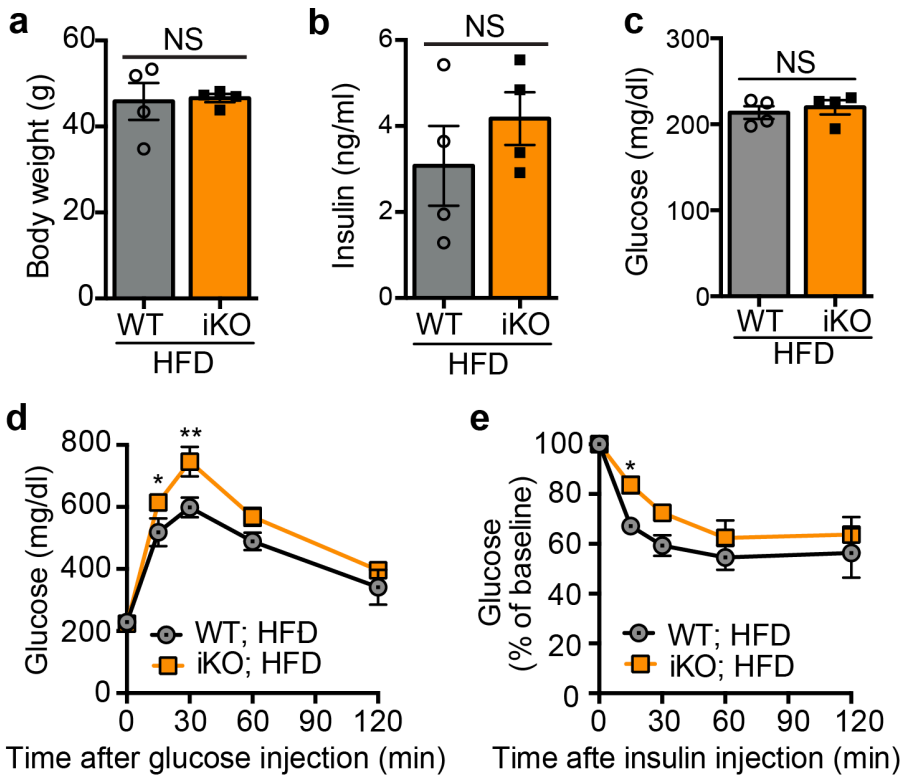

Supplementary Figure 3. BMPER depletion exacerbates glucose responses in HFD-fed mice. Metabolic studies were performed with BMPER iKO and WT mice following eight weeks of HFD feeding. (**a**) Body weight. (**b-c**) Fasted insulin and glucose. (**d-e**) Glucose and insulin tolerance tests. HFD, high-fat diet. n= 4 (**a-e**). *, $P< 0.05$. **, $P< 0.01$. NS, not significant.

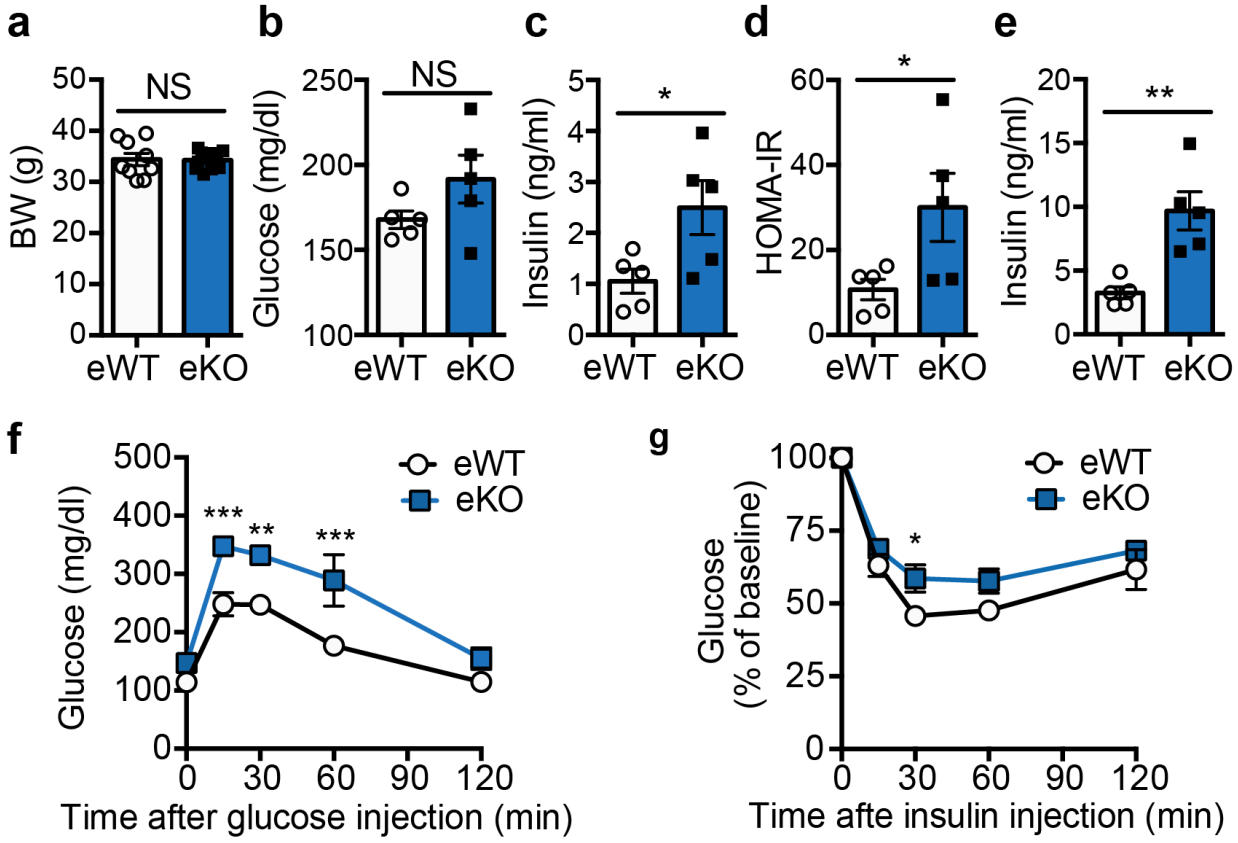

Supplementary Figure 4. BMPER depletion in ECs leads to glucose dysregulation. Metabolic studies were performed with BMPER eKO and eWT mice at four months after tamoxifen injection. (**a**) Body weight (BW). (**b-d**) Fasted glucose and insulin, HOMA-IR. (**e**) Fed insulin. (**f-g**) Glucose and insulin tolerance tests. eWT, BMPER$^{flox/flox}$; Cdh5-CreER$^{-/-}$. eKO, BMPER$^{flox/flox}$; Cdh5-Cre ER$^{+/-}$. n=5 (**a-g**). *, $P< 0.05$. **, $P< 0.01$. ***, $P< 0.001$. NS, not significant.

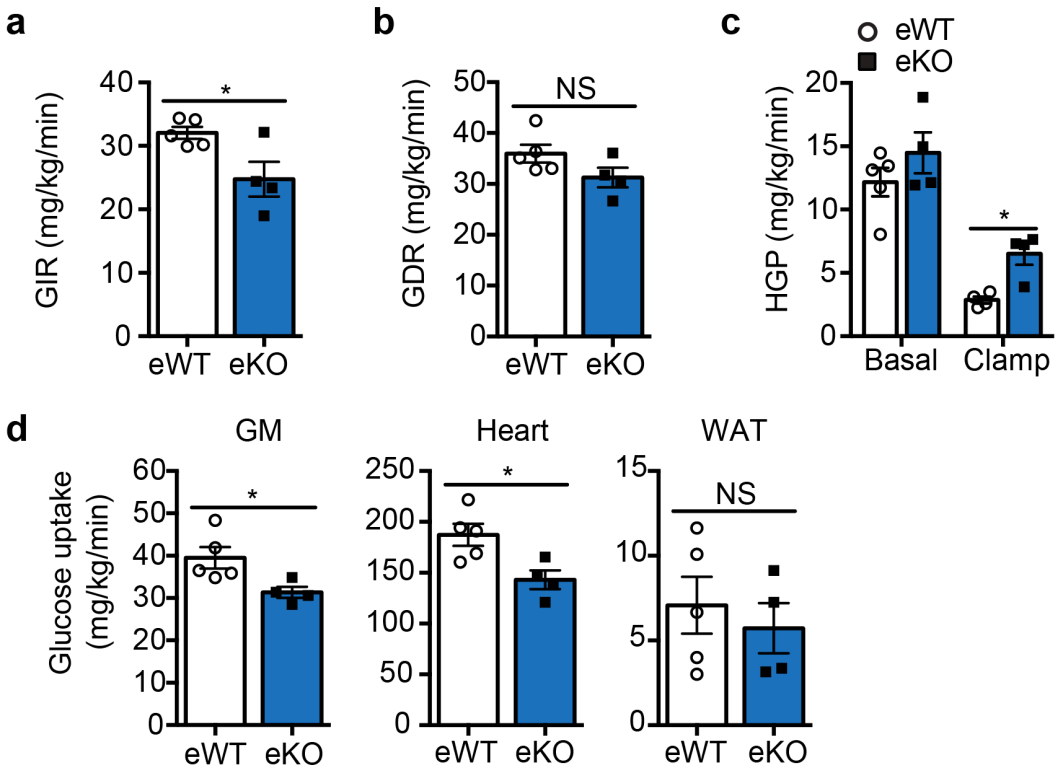

Supplementary Figure 5. BMPER depletion in ECs leads to insulin resistance. Clamp studies were performed with BMPER eKO and eWT mice at four months after tamoxifen injection. (**a**) Glucose infusion rate (GIR). (**b**) Glucose disposal rate (GDR). (**c-d**) Hepatic glucose production (HGP; **c**) and glucose uptake in peripheral tissues (**d**) were analyzed with hyperinsulinemic-euglycemic clamps. GM, gastrocnemius muscle; WAT, white adipose tissue. n=5 (**a-d**). *, $P< 0.05$. NS, not significant.

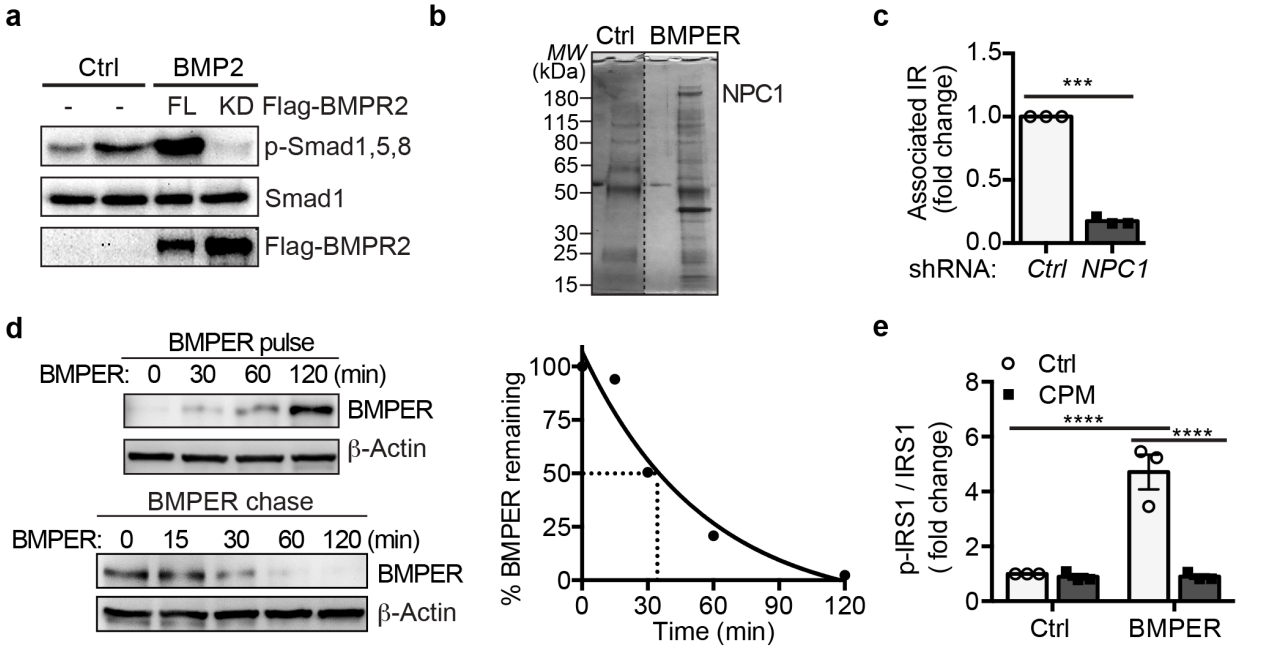

Supplementary Figure 6. The regulation of BMPER-promoted insulin signaling pathway. Hepatocytes were transduced with adenovirus of flag-tagged BMPR2 full length (FL) or kinase-dead mutant (KD). Cells were then treated with BMP2 (4 nM, 1 hr). (**b**) NPC1 was identified in BMPER-bound complex. HEK293 cells were treated with BMPER (30 nM) and lysates were immunoprecipitated with anti-BMPER antibody and stained with Coomassie blue. Selected bands were subjected for mass spectrometry analysis. (**c**) Quantitative data for Figure 4e. (**d**) Hepatocytes were pulsed with Flag-BMPER (100 nM, 7.2 ng) for indicated time periods (left top panel), and then chased at 4°C (left bottom panel). Right panel is graphic representation of normalized intracellular BMPER level from the cold chase. (**e**) Quantitative data for Figure 4h. n=3 (**c, e**). ***, $P< 0.001$. ****, $P< 0.0001$.

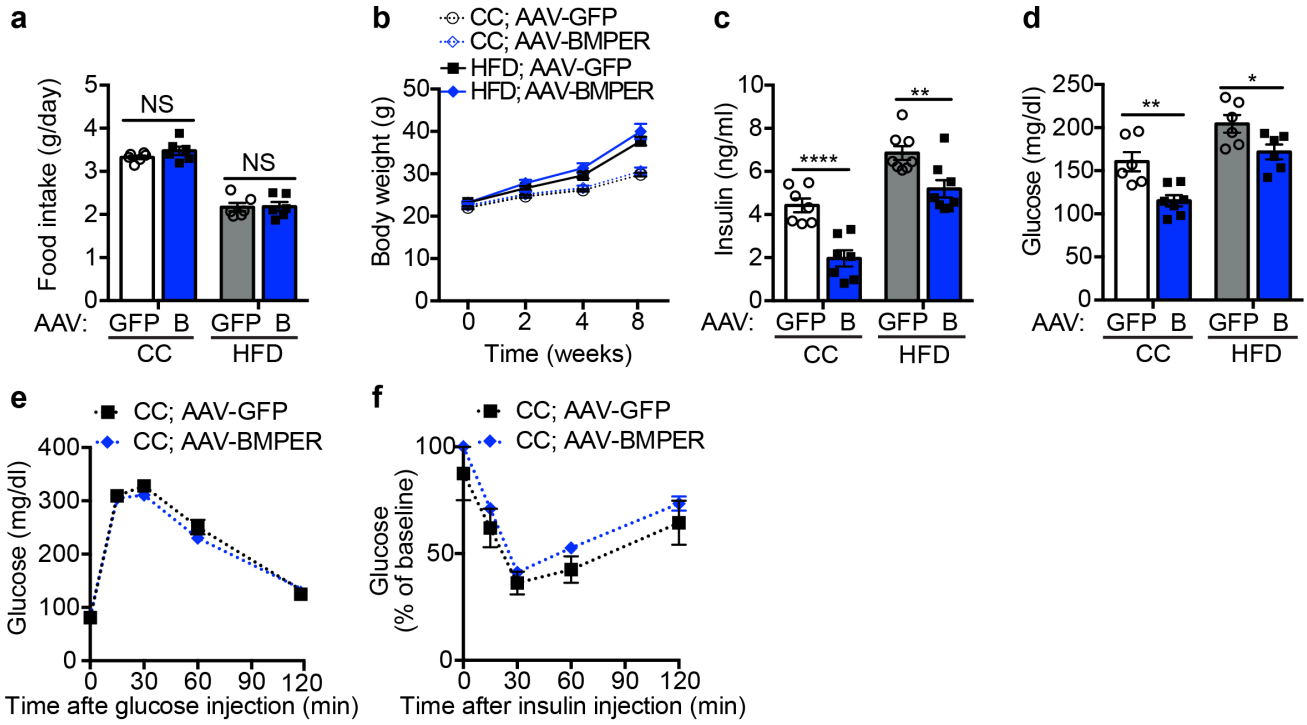

Supplementary Figure 7. AAV-BMPER improves glucose responses in DIO mice. AAV-BMPER or AAV-GFP was injected into C57BL/6 mice and then fed them HFD for eight weeks. (**a**) Food intake in AAV-GFP or AAV-BMPER (B) injected mice that were fed HFD or CC diet. (**b**) Body weight. (**c-d**) Fed insulin and glucose. (**e-f**) Glucose and insulin tolerance tests. n=6 (**a**), 8 (**b-f**). *, $P< 0.05$. **, $P< 0.01$. ****, $P< 0.0001$. NS, not significant.

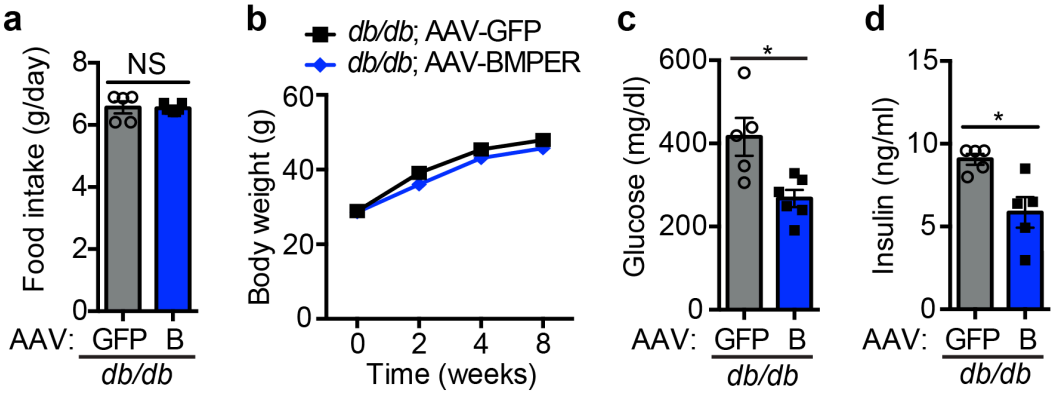

Supplementary Figure 8. AAV-BMPER improves glucose responses in *db/db* mice. AAV-BMPER or AAV-GFP was injected into 5-week-old *db/db* mice and then monitored for eight weeks. (**a**) Food intake in AAV-GFP or AAV-BMPER (B)- injected *db/db* mice. (**b**) Body weight. (**c-d**) Fed insulin and glucose. n=5 for AAV-GFP and 7 for AAV-BMPER group. *, $P< 0.05$. NS, not significant.